Nonlinear Fluctuating Hydrodynamics for 1 Dimensional Chains

Hashiam Kadhim

Contents

1 Introduction

In many cases, fluids in physical space can be modelled with anharmonic chains. The standard procedure for analysing such chains is to lift the Euler equations to the compressible Navier-Stokes equations which include friction by second order derivative terms. This provides the desired broadening behaviour of the chain on the linearised level. As a basic principle of statistical mechanics, dissipation (which in this case is obtained by the friction) is connected with fluctuations. Hence, at the linearized level of precision, the dynamical evolution equations are given by the linearized Navier-Stokes equations with added random currents, which are modelled as space-time white noise in order to capture the behaviour of the fluctuations. This theory is known as linear fluctuating hydrodynamics. In order to upgrade to non-linear fluctuating hydrodynamics, one must expand the Euler equations up to second order, with the hope that this will capture the super-diffusive broadening behaviour. This method assumes the existence of locally conserved fields.

The main goal of this paper is to outline a strategy to study the equilibrium time correlations of the conserved fields of an anharmonic chain through non-linear fluctuating hydrodynamics. In order to achieve this, we walk through the process using the BS model which is introduced in section 3 as the case study. In short, the strategy is to first identify the n conserved fields. The dynamics then have an n-parameter family of translation invariant steady states. The next step is to to compute the steady state average currents (which are functions of the steady state average of the conserved fields) in the form of Euler equations and expand these equations up to second order. Adding dissipation plus noise, along with a linear transformation allows us to end up with a two component stochastic Burgers equation, for which we can use section 2 to find the universality classes of the correlation functions.

2 Background Material

2.1 The Stochastic Burgers Equation

The stochastic burgers equation is given by:

$$\partial_t u_1 + \partial_x (c u_1 + G^1_{11} u_1^2 - D \partial_x u_1 + \sqrt{2D}\xi_1) = 0 \tag{1}$$

Where $D > 0$ is the viscosity, $c \in \mathbb{R}$ is the velocity of propagation, $G^1_{11} \in \mathbb{R}$ is the strength of the non linearity, and ξ_1 is a space time white noise with unit strength and correlation:

$$E[\xi(x,t)\xi(y,s)] = \delta(x-y)\delta(t-s) \tag{2}$$

The choice of subscripts and superscripts here is so that there's a natural generalization to a 2 dimensional case given below. It has been shown, for instance in [5] that spacial white noise with unit variance and mean zero is an invariant measure for (1). This paper will study the stationary process governed by the 2 dimensional version of (1). That is, we are interested in $\langle u_1(x,t)u_1(0,0)\rangle$ where in the 2 dimensional case, the subscript for u term could be either 1 or 2. Here $\langle\cdot\rangle$ refers to the expectation with respect to the stationary process. For the 1 dimensional case, an exact solution has been found in [6] which behaves as

$$\langle u_1(x,t)u_1(0,0)\rangle \simeq (\lambda_B t)^{-2/3} f_{\mathrm{KPZ}}((\lambda_B t)^{-2/3}(x-ct)) \tag{3}$$

for large x,t where $\lambda_B = 2\sqrt{2}|G^1_{11}|$. This validates previous non rigorous computations in [7]. The universal scaling function f_{KPZ} tabulated in [8] is shown to have the following properties: $f_{\mathrm{KPZ}} \geq 0$, $f_{\mathrm{KPZ}}(x) = f_{\mathrm{KPZ}}(-x)$,

$$\int_{\mathbb{R}} f_{\mathrm{KPZ}}(x)dx = 1, \int_{\mathbb{R}} x^2 f_{\mathrm{KPZ}}(x)dx = 0.510523... \tag{4}$$

In the 1 dimensional case, we could consider a frame of reference moving with velocity c. Then we can get rid of the cu_1 term in (1) since with relabelling of variables, it becomes equivalent to:

$$\partial_t u + \partial_x(\lambda u^2 - \nu\partial_x u - \sqrt{D'}\partial_x \xi) = 0 \tag{5}$$

(5) is formally equivalent to the KPZ equation

$$\partial_t h = -\lambda(\partial_x h)^2 + \nu\partial_x h + \sqrt{D'}\xi \tag{6}$$

since one equation can be solved from the other by $u = \partial_x h$. For instance, supposing h satisfies (6), and plugging $u = \partial_x h$ into (5), we get:

$$\begin{aligned} &\partial_t\partial_x h + \partial_x(\lambda(\partial_x u)^2 - \nu\partial_x\partial_x h - \sqrt{D'}\xi) \\ &= \partial_x\partial_t h + \partial_x(\lambda(\partial_x u)^2 - \nu\partial_x^2 h - \sqrt{D'}\xi) \\ &= \partial_x(-\lambda(\partial_x h)^2 + \nu\partial_x h + \sqrt{D'}\xi) + \partial_x(\lambda(\partial_x u)^2 - \nu\partial_x^2 h - \sqrt{D'}\xi) \\ &= 0 \end{aligned} \tag{7}$$

Of course we are assuming the nice condition that h is differentiable with respect to the spatial variable.

In the case of $\overrightarrow{u} = (u_1, u_2)$, the two dimensional stochastic Burgers equation becomes:

$$\partial_t u_\alpha + \partial_x(c_\alpha u_\alpha + \overrightarrow{u}\cdot G^\alpha \overrightarrow{u} - \partial_x(D\overrightarrow{u})_\alpha + (\sqrt{2D}\xi)_\alpha) = 0,\ \ \alpha = 1,2 \tag{8}$$

where c_α is the propagation velocity of the α-th component, the symmetric matrices $G^\alpha \in \mathbb{R}^{2\times 2}$ determine the strength of nonlinearity, the symmetric positive matrix $D \in \mathbb{R}^{2\times 2}$ represents the diffusion matrix, and the noise $\overrightarrow{\xi}$ is a vector of two independent mean zero Gaussian white noises with covariance $E[\xi_\alpha(x,t)\xi_{\alpha'}(y,s)] = \delta_{\alpha\alpha'}\delta(x-y)\delta(t-s)$. In the case of $G^1_{22} = G^2_{12}$ and $G^2_{11} = G^1_{12}$, the invariant measure is known to be a spacial white noise with independent components.

In (1), we mentioned that we can change the coordinate system to eliminate the term with propagation velocity so that it is in a form like (5). In the case of (8) however, one could in general only eliminate one of the $c_\alpha u_\alpha$ terms with a change of coordinate system, and so the relative velocity persists. The covariance matrix becomes $\langle u_\alpha(x,t)u_{\alpha'}(0,0)\rangle$. In the linear case $G^1 = G^2 = 0$, if $c_1 \neq c_2$, then for large x, t, the covariance consists of two decoupled Gaussian peaks centred at $c_\alpha t$ with width $\sqrt{D_{\alpha\alpha} t}$. The cross terms of D do not matter in this case since the two peaks move with distinct velocities. In the non-linear case, this property also holds to a certain extent. The linear drift term is dominant and so the two equations in (8) decouple for large x, t. It will be made more precise in section 4 that:

$$\langle u_\alpha(x,t)u_{\alpha'}(0,0)\rangle \simeq \delta_{\alpha\alpha'} f_\alpha(x,t) \tag{9}$$

where $f_\alpha(x,0) = \delta(x)$ and f_α satisfies the memory equation:

$$\begin{aligned} \partial_t f_\alpha(x,t) =& (-c_\alpha \partial_x + D_{\alpha\alpha}\partial_x^2) f_\alpha(x,t) \\ &+ \int_0^t ds \int_{\mathbb{R}} dy \partial_y^2 M_{\alpha\alpha}(y,s) f_\alpha(x-y, t-s) \end{aligned} \tag{10}$$

where $D_{\alpha\alpha}$ are the diagonal terms of the diffusion matrix and $M_{\alpha\alpha}$ is the memory kernel:

$$M_{\alpha\alpha}(x,t) = 2 \sum_{\alpha',\alpha''=1}^{2} (G^\alpha_{\alpha'\alpha''})^2 f_{\alpha'}(x,t) f_{\alpha''}(x,t) \tag{11}$$

$$\simeq 2 \sum_{\alpha'=1}^{2} (G^\alpha_{\alpha'\alpha'})^2 f_{\alpha'}(x,t)^2 \tag{12}$$

2.2 Classification of the Two-Component Stochastic Burgers Equation

Except for a few cases, the exact asymptotic behaviour of f_α is not known. Hence educated scaling ansatz are made for f_α. The type scaling predicted is organized in tables 1,2,3 and depends on whether $G^\alpha_{\alpha'\alpha''}$ vanishes or not. In the tables below, KPZ indicates the KPZ scaling described in (3). The "α-Levy" scaling is determined by the maximally asymmetric α-stable law with exponent α which is described more in section 4.2. The "*gold*-Levy" case is just the "α-Levy" scaling, where $\alpha = (1+\sqrt{5})/2 \simeq 1.618$ is the golden mean. Finally, the "diff" scaling stands for diffusive, is a Gaussian peak with width proportional to $\sqrt{t}$.

Table 1: $G^1_{11} \neq 0, G^2_{22} \neq 0$	f_1	f_2
$G^1_{22} = 0$ or $G^1_{22} \neq 0$, $G^2_{11} = 0$ or $G^2_{11} \neq 0$	KPZ	KPZ

In the case above, the KPZ scaling function is not an exact solution, but it's very close to the exact solution. This is discussed in detail in [9].

Table 2: $G^1_{11} \neq 0, G^2_{22} = 0$	f_1	f_2
$G^1_{22} = 0$ or $G^1_{22} \neq 0$, $G^2_{11} \neq 0$	KPZ	$\frac{5}{3}$-Levy
$G^1_{22} \neq 0$, $G^2_{11} = 0$	modified KPZ	diff
$G^1_{22} = 0$, $G^2_{11} = 0$	KPZ	diff

Expanding the term with G^α in (8), it becomes: $G^\alpha_{11}u_1^2 + G^\alpha_{12}u_1u_2 + G^\alpha_{21}u_1u_2 + G^\alpha_{22}u_2^2$. In the case above where $G^2_{11} \neq 0$, the KPZ peak for f_1 feeds into f_2 to generate a peak with $\frac{5}{3}$-Levy asymptotic, but since $G^2_{22} = 0$, and $G^2_{11} \neq 0$, the effect of f_2 on f_1 is negligible so it stays KPZ. In the case where $G^2_{11} = 0$ and $G^1_{22} = 0$, f_2 is diffusive since it's close to the case where $G^2 = 0$. In the case of $G^2_{11} = 0$ and $G^1_{22} \neq 0$, peak 2 has increased feedback onto peak 1 which also has dynamical exponent $z = 3/2$, so it's predicted to have a modified KPZ scaling.

Table 3: $G^1_{11} = 0, G^2_{22} = 0$	f_1	f_2
$G^1_{22} \neq 0$, $G^2_{11} \neq 0$	*gold*-Levy	*gold*-Levy
$G^1_{22} \neq 0$, $G^2_{11} = 0$	$\frac{3}{2}$-Levy	diff
$G^1_{22} = 0$, $G^2_{11} \neq 0$	diff	$\frac{3}{2}$-Levy
$G^1_{22} = 0$, $G^2_{11} = 0$	diff	diff

The *gold*-Levy case above is used for an example computation in section 4.1. The diffusion peaks are as expected because they follow the same pattern from table 2, that is, if $G^\alpha_{\alpha\alpha} = 0$ and $G^\alpha_{\beta\beta} = 0$ where $\alpha \neq \beta$, then we can expect a diffusive peak for f_α. The last case is when $G^\alpha_{\beta\beta} \neq 0$ where we get that the diffusive peak feeds into the α peak causing it to be $\frac{3}{2}$-Levy.

In order to relate these equations to a physical model, the model must have exactly 2 conserved quantities or conservation laws and the dynamics should be sufficiently chaotic in order to have good space-time mixing properties. If there were more conserved quantities, the following approach will likely miss some of the dynamics. Once a model is approximated well with an equation of the form (8), one could discern the universality class under consideration. This would be hard to guess just by inspection. Below we walk through this process with one such model.

3 One Dimensional Fluctuating Hydrodynamics

3.1 BS model with Two Conserved Fields

The Bernadin-Stoltz model (called "*BS* model" for short) was motivated by anharmonic chains and first introduced in [2]. Let V be a potential in $\mathbb{R}$. Consider the real valued field $(\eta_i)_{i\in\mathbb{Z}}$ where each η_i is real valued. The dynamics of this field consist of a deterministic and stochastic part. For some finite integer N, we define $\boldsymbol{\eta} = (\eta_0, ..., \eta_{N-1})$ to be the displacement field, and impose periodic boundary conditions $\eta_i = \eta_{i+N}$. It is equivalent and sometimes more helpful to think of the dynamics of $\boldsymbol{\eta}$ over the discrete torus $\mathbb{T}_N = \mathbb{R}/N\mathbb{Z}$ of length N.

The deterministic part is given by:

$$\frac{d}{dt}\eta_i = V'(\eta_{i+1}) - V'(\eta_{i-1}) \tag{13}$$

It is at this point that we add the condition that $V(\eta_i) + \eta_i$ is at least bounded from below or from above $\forall i$. We will use this condition in equations (16)-(18) below. The stochastic part consists of neighbouring displacements being exchanged at independent random times distributed according to an exponential law with parameter γ. Taking into account the boundary conditions, the dynamics of the deterministic part and stochastic part, it is clear that:

$$\sum_{i=0}^{N-1} \frac{d}{dt}\eta_i = \sum_{i=0}^{N-1} [V'(\eta_{i+1}) - V'(\eta_{i-1})] = 0 \tag{14}$$

and

$$\sum_{i=0}^{N-1} \frac{d}{dt}V(\eta_i) = \sum_{i=0}^{N-1} [V'(\eta_i)V'(\eta_{i+1}) - V'(\eta_i)V'(\eta_{i-1})] = 0 \tag{15}$$

Hence the displacement field $\boldsymbol{\eta}$ and the (potential) energy field $V(\boldsymbol{\eta})$ is conserved. In other words, the volume which we denote by $\sum_{i=0}^{N-1} \eta_i$ and energy which we denote by $\sum_{i=0}^{N-1} V(\eta_i)$ is constant. Consequently, the two-parameter family of measures defined by:

$$\mu_{\lambda,\beta}(d\eta_0, ..., d\eta_{N-1}) = Z_{\lambda,\beta}^{-1} \prod_{i=0}^{N-1} e^{-\beta(V(\eta_i)+\lambda\eta_i)} d\eta_i \tag{16}$$

$$= Z_{\lambda,\beta}^{-1} \exp\left[-\beta(\sum_{i=0}^{N-1} V(\eta_i) + \lambda \sum_{i=0}^{N-1} \eta_i)\right] d\eta_i \tag{17}$$

is invariant, where the parameters $\beta > 0$ and $\tau \in \mathbb{R}$ are called chemical potentials. Along with the condition on V above, the admissible values of λ might be restricted so that the normalization constant

$$Z_{\lambda,\beta} = \prod_{i=0}^{N-1} \int_{-\infty}^{\infty} e^{-\beta(V(x)+\lambda x)} dx \tag{18}$$

will converge. The generator for the deterministic part is given by

$$\mathcal{A}_N = \sum_{i=0}^{N-1} [V'(\eta_{i+1}) - V'(\eta_{i-1})]\partial_{\eta_i} \tag{19}$$

Thus the following microscopic volume and energy conservation laws hold for the deterministic part (written in terms of currents):

$$\frac{d}{dt}\begin{pmatrix} \eta_i \\ V(\eta_i) \end{pmatrix} = \mathcal{A}_N \begin{pmatrix} \eta_i \\ V(\eta_i) \end{pmatrix} = -\nabla J^{i-1,i} = J^{i,i+1} - J^{i-1,i} \tag{20}$$

where ∇ is the discrete gradient (for a function $f : \mathbb{Z} \to \mathbb{R}$, $\nabla f(x) = f(x+1) - f(x)$) and

$$J^{i,i+1} := \begin{pmatrix} J_v^{i,i+1} \\ J_e^{i,i+1} \end{pmatrix} = - \begin{pmatrix} V'(\eta_i) + V'(\eta_{i+1}) \\ V'(\eta_i)V'(\eta_{i+1}) \end{pmatrix} \tag{21}$$

For now we take a small detour to talk about the case of three conserved fields, as well as to outline rigorously what we mean by the macroscopic limit. In short, one just has to know that the macroscopic limit is the limit $N \to \infty$ with space being normalized by N^{-1} and macroscopic time scaling tN. The macroscopic setting is denoted by using the continuous spacial variable x instead of the discrete one j. In order continue reading without this detour, you may skip to section 3.4.

3.2 The case of Three Conserved Fields

The purpose of this section is to introduce a model with 3 conserved fields. Clearly the theory in section 2 is not enough to tackle this problem, however the other sections can be adapted. That is, the strategy of non-linear fluctuating hydrodynamics is the same, but discerning the universality class at the end depends on the classification of a 3 component stochastic Burgers equation. Such study can be found in [2] and [3]. Consider N particles with positions q_j and momenta p_j where $j = 0, ..., N-1$. The particles are coupled through a potential, which we apply similar restraints to (as in the previous section), and give the Hamiltonian:

$$H = \sum_{j=0}^{N-1} \big(\frac{1}{2}p_j^2 + V(q_{j+1} - q_j)\big) \tag{22}$$

With similar boundary condition: $q_{1+N} = q_1$. Implying equations of motion:

$$\frac{d^2}{dt^2} q_j = V'(q_{j+1} - q_j) - V'(q_j - q_{j-1}) \tag{23}$$

Letting $r_j = q_{j+1} - q_j$ be the positional difference, we obtain the equations of motion:

$$\dot{r}_j = \dot{q}_{j+1} - \dot{q}_j = \partial_{p_{j+1}} H - \partial_{p_j} H = p_{j+1} - p_j, \quad p_1 = p_{1+N} \tag{24}$$

$$\dot{p}_j = V'(r_j) - V'(r_{j-1}) \quad r_{-1} = r_{N-1} \tag{25}$$

Through (24) there is coupling with the right neighbour, and (25) there is coupling with the left neighbour. Letting $e_j = \frac{1}{2}p_j^2 + V(r_j)$ be the energy, we see that:

$$\frac{d}{dt} \sum_{j=1}^{N-1} r_j = 0, \quad \frac{d}{dt} \sum_{j=1}^{N-1} p_j = 0 \tag{26}$$

$$\frac{d}{dt}\sum_{j=1}^{N-1} e_j = \frac{d}{dt}\sum_{j=1}^{N-1} p_{j+1}V'(r_j) - p_jV'(r_{j-1}) = 0 \tag{27}$$

Hence, the elongation, momentum, and energy fields are conserved respectively. We can also add the same random nearest neighbour exchange in the BS model and still have these fields be conserved due to translation invariance. In fact, because this randomness that conserves these fields is added, these are the "only" conserved quantities for the dynamics in the infinite long chain limit $N \to \infty$. When studying the time dependent statistical correlations between the modes, one has to study the interactions between the conserved modes. If one were to neglect a conserved field, they would likely miss some of these dynamical processes.

The theory in section 3 and 4 can be adapted to this model, or many other anharmonic chain models. We will use the BS model as the main one, and walk through the analysis for that specific model. However it is important to note that these techniques can be used in much the same way for different models. In order to proceed for this model, we would start with the same analysis in section 3.1. The difference being that the currents (20) have 3 components, and the general family of invariant measures (16) depends on 3 parameters instead of 2. That is, (20) − (21) is replaced by:

$$\frac{d}{dt}\begin{pmatrix} r_i(t) \\ p_i(t) \\ e_i(t) \end{pmatrix} = J^{i+1,t} - J^{i-1,t} \tag{28}$$

Where the 3 component current becomes

$$J^{i,t} := -\begin{pmatrix} p_i(t) \\ V'(r_{i-1}(t)) \\ p_iV'(r_{i-1}(t)) \end{pmatrix} \tag{29}$$

As we move forward with the analysis of the BS model, it is helpful to keep in mind how one would use the same techniques with this model. The beginning of section 4 is general enough to apply to all models once the appropriate preparation has been made (as the reader will see in section 3.4).

3.3 Macroscopic Limit

The goal of this section is to make rigorously precise the definition of the macroscopic limit. In short, we study the macroscopic limit $N \to \infty$ with space being normalized by N^{-1} and macroscopic time scaling tN. In order to be precise, we must introduce many definitions. This treatment is identical to, and first presented in [2]. First we define the mean volume and mean energy with respect to the stationary measure:

$$v(\lambda, \beta) = \mathbb{E}_{\mu_{\lambda,\beta}}[\eta_i] = -\partial_\lambda\big(\log Z_{\lambda,\beta}\big) \tag{30}$$

$$e(\lambda, \beta) = \mathbb{E}_{\mu_{\lambda,\beta}}[V(\eta_i)] = -\partial_\beta\big(\log Z_{\lambda,\beta}\big) \tag{31}$$

where $Z_{\lambda,\beta}$ is the partition function defined in (18). Note that $e > 0$ since the potential is non-negative. These relations can be inverted to express λ and β in terms of e and v. First define the thermodynamic entropy $S : (0, \infty) \times \mathbb{R} \to [-\infty, \infty)$ by:

$$S(e, v) = \inf_{\lambda\in\mathbb{R},\beta>0} \left\{ \lambda v + \beta e + \log Z_{\lambda,\beta} \right\} \tag{32}$$

Let $\mathcal{U}$ be the convex subset of $(0, \infty) \times \mathbb{R}$ where $S(e, v) > -\infty$. Let $\mathring{\mathcal{U}}$ be the interior of $\mathcal{U}$. Then for any $(e, v) \in \mathring{\mathcal{U}}$, we can isolate for the chemical potentials by:

$$\lambda(e, v) = (\partial_v S)(e, v), \qquad \beta(e, v) = (\partial_e S)(e, v) \tag{33}$$

Next define the tension by

$$\tau(\lambda, \beta) := -\mathbb{E}_{\mu_{\lambda,\beta}}[V'(\eta_i)] = \lambda/\beta \tag{34}$$

and hence

$$\mathbb{E}_{\mu_{\lambda,\beta}}[V'(\eta_i)V'(\eta_{i+1})] = \tau^2 \tag{35}$$

Hence we can write the tension $\tau(e, v)$ to mean $\tau(\lambda(e, v), \beta(e, v))$.

Now we can start describing the macroscopic limit. We write $Z_{\lambda,\beta} = Z(\lambda, \beta)$. We assume that the system is initially distributed according to a local Gibbs equilibrium state $X_0 : \mathbb{T} \to \mathring{\mathcal{U}}$, $X_0 = \begin{pmatrix} \mathfrak{v}_0 \\ \mathfrak{e}_0 \end{pmatrix}$.

That is, the initial state of the system of size N is described by:

$$\mu^N_{\mathfrak{v}_0,\mathfrak{e}_0}(d\boldsymbol{\eta}) = \prod_{i\in\mathbb{T}_N} \frac{e^{-\beta_0(i/N)V(\eta_i)+\lambda_0(i/N)\eta_i)}}{Z(\lambda_0(i/N), \beta_0(i/N))} d\eta_i \tag{36}$$

Where $\lambda_0(\mathfrak{e}_0(x), \mathfrak{v}_0(x)) = \lambda(x), \beta(\mathfrak{e}_0(x), \mathfrak{v}_0(x)) = \beta_0(x)$. The system at time t is denoted by

$$X(t, \cdot) = \begin{pmatrix} \mathfrak{v}(\mathfrak{t}, \cdot) \\ \mathfrak{e}(\mathfrak{t}, \cdot) \end{pmatrix} \tag{37}$$

Taking expectations of both sides of $(20) - (21)$ and using $(34) - (35)$, we see that the system satisfies the expected partial differential equations:

$$\partial_t \begin{pmatrix} \mathfrak{v}(t, x) \\ \mathfrak{e}(t, x) \end{pmatrix} + \partial_x \begin{pmatrix} 2\tau(\mathfrak{v}(t, x), \mathfrak{e}(t, x)) \\ -[\tau(\mathfrak{v}(t, x), \mathfrak{e}(t, x))]^2 \end{pmatrix} = 0 \tag{38}$$

In a sense we are zooming out so that the discrete system becomes continuous (hence x replacing N). For completeness, we give 1 more definition necessary for the theorem even though the idea of the macroscopic limit has been set. For continuous functions $G, H : \mathbb{T} \to \mathbb{R}$, their empirical average with respect to the volume-energy measure is defined by:

$$\begin{pmatrix} \mathcal{E}_N(t, G) \\ \mathcal{V}_N(t, H) \end{pmatrix} = \begin{pmatrix} \frac{1}{N} \sum_{x \in \mathbb{T}_N} G(x/N) V(\eta_x(t)) \\ \frac{1}{N} \sum_{x \in \mathbb{T}_N} V(x/N) \eta_x(t) \end{pmatrix} \tag{39}$$

Finally, we can state the macroscopic limit theorem:

Theorem 3.1 (Macroscopic Limit theorem [2]). *Fix some $\gamma > 0$ and consider the dynamics on the torus $\mathbb{T}_N$ given by our model. Assume that the system is initially distributed according to a local Gibbs state* (36) *with smooth energy profile $\mathfrak{e}_0$ and volume profile $\mathfrak{v}_0$. Consider a poisitive time t such that the solution $(\mathfrak{e}, \mathfrak{v})$ to* (38) *belongs to $\mathring{\mathcal{U}}$ and is smooth on the time interval $[0, t]$. Then for any continuous test functions $G, H : \mathbb{T} \to \mathbb{R}$, the following convergence in probability holds as $n \to \infty$:*

$$\Big(\mathcal{E}_N(tN, G), \mathcal{V}_N(tN, H) \Big) \to \Big(\int_{\mathbb{T}} G(q) \mathfrak{e}(t, q) dq, \int_{\mathbb{T}} H(q) \mathfrak{v}(t, q) dq \Big) \tag{40}$$

3.4 Comparing to Stochastic Burgers and computing non-linear couplings

The main point of this section is analysing the macroscopic dynamics (38) by writing it in the form of the two-component stochastic Burgers equation (5). First, we make a slight change of convention: define the stationary measure $\nu_{\tau,\beta}$ to by

$$\nu_{\tau,\beta}(d\eta_0, ..., d\eta_{N-1}) = Z_{\tau,\beta}^{-1} \prod_{i=0}^{N-1} e^{-\beta(V(\eta_i) + \tau\eta_i)} d\eta_i \tag{41}$$

it is identical to $\mu_{\lambda,\beta}$ but with chemical potentials re-factored so that we conveniently have:

$$-\mathbb{E}_{\nu_{\tau,\beta}}[V'(\eta_i)] = (\tau\beta)/\beta = \tau \tag{42}$$

and

$$\mathbb{E}_{\nu_{\tau,\beta}}[V'(\eta_i) V'(\eta_{i+1})] = \tau^2 \tag{43}$$

Hence τ can be considered as a function of the average volume and energy

$$\mathbb{E}_{\nu_{\tau,\beta}}[\eta_i] = v_{\tau,\beta} \tag{44}$$

and

$$\mathbb{E}_{\nu_{\tau,\beta}}[V(\eta_i)] = e_{\tau,\beta} \tag{45}$$

Now letting $\langle \cdot \rangle_{\tau,\beta} = \langle \cdot \rangle$ be the average in the stationary process with starting measure $\nu_{\tau,\beta}$, we wish to study the covariance matrix of the conserved fields in the limit of taking an infinitely long chain.

$$S_{\alpha,\alpha'}(j,t) = \langle g_\alpha(\eta_{j,t}) g_{\alpha'}(\eta_{0,0}) \rangle_{\tau,\beta} - \langle g_\alpha(\eta_{j,t}) \rangle_{\tau,\beta} \langle g_{\alpha'}(\eta_{0,0}) \rangle_{\tau,\beta} \tag{46}$$

where $g_1(\eta) = \eta$, $g_2(\eta) = V(\eta)$.

We begin by linearising the Euler equations (38) around a uniform background profile (v_0, e_0) by writing $v(x,t) = v_0 + \tilde{v}(x,t)$, $e(x,t) = e_0 + \tilde{e}(x,t)$. The correlator S should be governed by the following Euler equations up to a linear order:

$$\partial_t \begin{pmatrix} v(t,x) \\ e(t,x) \end{pmatrix} + \partial_x \begin{pmatrix} 2\tau(v(t,x), e(t,x)) \\ -[\tau(v(t,x), e(t,x))]^2 \end{pmatrix} \tag{47}$$

$$\approx \partial_t \begin{pmatrix} \tilde{v}(t,x) \\ \tilde{e}(t,x) \end{pmatrix} + \begin{pmatrix} 2\frac{\partial \tau(v_0,e_0)}{\partial v} \frac{\partial \tilde{v}}{\partial_x} + 2\frac{\partial \tau(v_0,e_0)}{\partial e} \frac{\partial \tilde{e}}{\partial x} \\ -2\tau(v_0,e_0)\frac{\partial \tau(v_0,e_0)}{\partial v} \frac{\partial \tilde{v}}{\partial_x} - 2\tau(v_0,e_0)\frac{\partial \tau(v_0,e_0)}{\partial e} \frac{\partial \tilde{e}}{\partial x} \end{pmatrix} \tag{48}$$

$$= \partial_t \begin{pmatrix} \tilde{v}(t,x) \\ \tilde{e}(t,x) \end{pmatrix} + 2 \begin{pmatrix} \partial_v \tau(v_0,e_0) & \partial_e \tau(v_0,e_0) \\ -\tau(v_0,e_0)\partial_v \tau(v_0,e_0) & -\tau(v_0,e_0)\partial_e \tau(v_0,e_0) \end{pmatrix} \partial_x \begin{pmatrix} \tilde{v}(t,x) \\ \tilde{e}(t,x) \end{pmatrix} \tag{49}$$

$$:= \partial_t \begin{pmatrix} \tilde{v}(t,x) \\ \tilde{e}(t,x) \end{pmatrix} + A(v_0,e_0)\partial_x \begin{pmatrix} \tilde{v}(t,x) \\ \tilde{e}(t,x) \end{pmatrix} \tag{50}$$

Letting $A := A(v_0, e_0)$, The above line becomes:

$$\partial_t \begin{pmatrix} \tilde{v}(t,x) \\ \tilde{e}(t,x) \end{pmatrix} + \partial_x \left[A \begin{pmatrix} \tilde{v}(t,x) \\ \tilde{e}(t,x) \end{pmatrix} \right] \tag{51}$$

Below, we will see that it is important to make the transformation $RAR^{-1} = K$ where $K = \begin{pmatrix} c & 0 \\ 0 & 0 \end{pmatrix}$ is the diagonal matrix of eigenvalues of A and R is obtained from the eigenvectors of A. This is because we wish to make (51) look like the two component stochastic Burgers equation (5). We can also transform the correlator directly by:

$$S^{\#}_{\alpha,\alpha'}(j,t) := (RSR^T)_{\alpha,\alpha'}(j,t) \tag{52}$$

Thus at the current rough linear approximation, the correlator $S^{\#} = \begin{pmatrix} f_1 & 0 \\ 0 & f_2 \end{pmatrix}$ is diagonal and satisfies

$$\partial_t S^{\#}_{\alpha,\alpha}(j,t) + \nabla(DS^{\#}_{\alpha,\alpha}(j,t)) = \partial_t S^{\#}_{\alpha,\alpha}(j,t) + c_\alpha(S^{\#}_{\alpha,\alpha}(j+1,t) - S^{\#}_{\alpha,\alpha}(j,t))) = 0 \tag{53}$$

where ∇ is the discrete gradient introduced in (20) and $c_1 = c, c_2 = 0$.

Expanding the currents (47) to second order, and letting $\overrightarrow{u} = (\tilde{v}, \tilde{e})$ and $H^{\gamma}_{\alpha,\beta} = \partial_{u_\alpha}\partial_{u_\beta} j_\gamma$ be the Hessian of the currents in (47) evaluated at the equilibrium parameters v_0, e_0, That is $j_v = 2\tau$, $j_e = -\tau^2$. the dynamics become:

$$0 = \partial_t \begin{pmatrix} \tilde{v}(t,x) \\ \tilde{e}(t,x) \end{pmatrix} + \partial_x \left[A \begin{pmatrix} \tilde{v}(t,x) \\ \tilde{e}(t,x) \end{pmatrix} + \frac{1}{2} \sum_{\alpha,\beta=1}^{2} H_{\alpha,\beta} u_\alpha u_\beta \right] \tag{54}$$

$$= \partial_t \overrightarrow{u} + \partial_x \left[A\overrightarrow{u} + \frac{1}{2} \langle \overrightarrow{u}, H\overrightarrow{u} \rangle \right] \tag{55}$$

Adding dissipation plus noise, we obtain the two component Langevin equation

$$\partial_t u_\alpha + \partial_x \left[(A\overrightarrow{u})_\alpha + \frac{1}{2} \langle \overrightarrow{u}, H^\alpha \overrightarrow{u} \rangle - \partial_x (\tilde{D}\overrightarrow{u})_\alpha + (\tilde{B}\overrightarrow{\xi})_\alpha \right] = 0 \tag{56}$$

Where $\alpha = 1, 2$. This is identical to the two component stochastic Burgers equation except for the fact that the linear drift term is not diagonal.

Therefore the next step is to make a linear transformation so that the velocity components in the above equation decouple and each one evolves with a definite velocity. This transformation is calculated from the left and right eigenvectors of A, act on the component space and will be denoted by R, so that $K := RAR^{-1} = \text{diag}(c, 0)$ where $c = 2(\partial_v - \tau\partial_e)\tau < 0$. We also require $RS(0,0)R^T = 1$ which amounts to requiring $R\overrightarrow{g}(j)$ to be uncorrelated in index. Transforming (56) by $\overrightarrow{\phi} = R\overrightarrow{u}$ we get:

$$\partial_t R^{-1}\phi_\alpha + \partial_x \left[(AR^{-1}\phi)_\alpha + \frac{1}{2} \langle R^{-1}\overrightarrow{\phi}, H^\alpha R^{-1}\overrightarrow{\phi} \rangle - \partial_x (\tilde{D}R^{-1}\phi)_\alpha + (\tilde{B}\overrightarrow{\xi})_\alpha \right] = 0 \tag{57}$$

Multiplying both sides by R from the left we obtain:

$$\partial_t \phi_\alpha + \partial_x \left[c_\alpha \phi_\alpha + \langle \overrightarrow{\phi}, G^\alpha \overrightarrow{\phi} \rangle - \partial_x (D\overrightarrow{\phi})_\alpha + (B\overrightarrow{\xi})_\alpha \right] = 0 \tag{58}$$

Where $R\tilde{D}R^{-1} = D$, $R\tilde{B} = B$, $RAR^{-1} = \text{diag}(c_1, c_2)$, with noise strength $BB^T = 2D$, and

$$G^\alpha = \frac{1}{2} \sum_{\alpha'=1}^{2} R_{\alpha,\alpha'} (R^{-1})^T H^{\alpha'} R^{-1} \tag{59}$$

If we define $\tilde{\phi}$ as the stationary process with mean 0 that satisfied (58), we can define the $\tilde{\phi} - \tilde{\phi}$ correlator by

$$S^{\#\phi}_{\alpha,\alpha'} = \langle \tilde{\phi}_\alpha(x,t) \tilde{\phi}_{\alpha'}(0,0) \rangle \tag{60}$$

One of the central conjectures of this study is that:

$$S^{\#}_{\alpha,\alpha'}(j,t) \simeq S^{\#\phi}_{\alpha,\alpha'}(x,t) \tag{61}$$

If the reader is interested in the computation R and G, it can be found in the appendix of [1] . $H^{\alpha'}$ written explicitly is given by:

$$H^v = \begin{pmatrix} \partial_v^2 j_h & \partial_v \partial_e j_h \\ \partial_v \partial_e j_h & -\partial_e^2 j_h \end{pmatrix} = 2 \begin{pmatrix} \partial_v^2 \tau & \partial_v \partial_e \tau \\ \partial_v \partial_e \tau & -\partial_e^2 \tau \end{pmatrix} \tag{62}$$

and

$$H^e = \begin{pmatrix} \partial_v^2 j_e & \partial_v \partial_e j_e \\ \partial_v \partial_e j_e & -\partial_e^2 j_e \end{pmatrix} = -\tau H^h - 2 \begin{pmatrix} (\partial_v \tau)^2 & \partial_v \tau \partial_e \tau \\ \partial_v \tau \partial_e \tau & -(\partial_e \tau)^2 \end{pmatrix} := -\tau H^h - 2\widehat{H^e} \tag{63}$$

Directly computing G^α from (59), it is found that the only non-zero entry of the heat mode coupling matrix G^2 is G^2_{11}. According to the classifications, there are two cases for the sound peak. The case of $G^1_{11} \neq 0$ gives us KPZ for the sound mode and $\frac{5}{3}$-Levy for the heat mode. The case $G^1_{11} = 0$ implies diffusive for the sound mode and $\frac{3}{2}$-Levy for the heat mode, however this case is highly unlikely, and equivalent to the condition that $(\partial_h - \tau\partial_e)\tau = 0$. Hence the second case is not considered standard. In section 5, numerical simulations for both cases are tested.

3.5 Scaling of the Sound and Heat Peaks

Here we state the scaling results relevant to the above calculations for the standard case. According to the classification in section 2.2, the sound peak (f_1) and heat peak (f_2) scale asymptotically like:

$$f_1(x,t) \simeq (\lambda_1 t)^{-2/3} f_{KPZ}((\lambda_1 t)^{-2/3}(x - ct)), \quad \lambda_1 = 2\sqrt{2}|G^1_{11}| \tag{64}$$

$$f_2(x,t) \simeq (\lambda_2 t)^{-3/5} f_{Levy,5/3,1}((\lambda_1 t)^{-3/5}(x - ct)), \quad \lambda_2 = a_h c^{-1/3} (G^2_{11})^2 \lambda_1^{-2/3} \tag{65}$$

where

$$a_h = \sqrt{3}\Gamma(\frac{1}{3}) \int_{\mathbb{R}} (f_{KPZ})^2 \simeq 1.81 \tag{66}$$

4 Mode Coupling Theory

In this section, we study (58) with n components instead of the 2 components obtained from the BS model. This is because the following theory can be made sufficiently general without much work. This section shows the derivation of a useful form of the time evolution of the modes.

We wish to move back and forth from the continuum limit and the discretized space, hence we indicate the setting by indices and variables. The continuous field $\phi(x,t)$ discretizes to $\phi_j(t)$, where $j = 0, ..., N-1$. Each $\phi_j(t)$ has components $\phi_{j,\alpha}(t)$ where $\alpha = 1, ..., n$ (in the BS model, we would have $\alpha = 1, 2$) as stated in the above paragraph. Let the spatial finite difference operator be denoted by $\nabla_{\#}$. That is $\nabla_{\#} f_j = f_j - f_{j-1}$ and with transpose $\nabla_{\#}^T f_j = f_j - f_{j+1}$. Then the discretized version of (58) reads:

$$\partial_t \phi_{j,\alpha} + \nabla_{\#}\left[c_\alpha \phi_\alpha + \mathcal{N}_{j,\alpha} - \nabla_{\#}^T D\phi_{j,\alpha} + \sqrt{2D}\xi_{j,\alpha}\right] = 0 \tag{67}$$

With periodic boundary conditions $\phi_j = \phi_{j+N}$, $\xi_j = \xi_{j+N}$ where $\xi_{j,\alpha}$ are independent Gaussian white noise with covariance

$$\langle \xi_{j,\alpha}(t)\xi_{j',\alpha'}(t')\rangle = \delta_{jj'}\delta_{\alpha\alpha'}\delta(t-t') \tag{68}$$

The diffusion matrix D acts on the components $(\phi_{j,1}, ..., \phi_{j,n})$ and the finite difference operator $\nabla_{\#}$ acts on the indices j. Finally $\mathcal{N}_{j,\alpha}$ is a quadratic term in ϕ. We will begin with the linear approximation $\mathcal{N}_{j,\alpha} = 0$ and then include the non-linear term later. In this approximation, since the drift is linear in ϕ, $\phi_{j,\alpha}(t)$ is a Gaussian process. Since the noise term is an independent Gaussian white noise, the Gaussian:

$$\prod_{j=1}^{N}\prod_{\alpha=1}^{n}\left(\frac{\exp[-\frac{1}{2}\phi_{j,\alpha}^2]}{\sqrt{2\pi}}d\phi_{j,\alpha}\right) = \rho_G \prod_{j=1}^{N}\prod_{\alpha=1}^{n} d\phi_{j,\alpha} \tag{69}$$

is an invariant measure. The extremal invariant measures are obtained by conditioning (69) on the hyperplanes

$$\sum_{j=1}^{N}\phi_{j,\alpha} = N_{\rho_\alpha} \tag{70}$$

which become independent Gaussians with mean ρ_α for large values of N. Let us fix $\rho_\alpha = 0$. Then the generator for (67) (remembering that for the time being we are setting $\mathcal{N}_{j,\alpha} = 0$) is:

$$L_0 = \sum_{j=0}^{N}\Bigg(- \sum_{\alpha=0}^{n} \nabla_{\#}(c_\alpha\phi_{j,\alpha} + \nabla_{\#}^T D\phi_{j,\alpha})\partial_{\phi_{j,\alpha}} + \sum_{\alpha,\beta=1}^{n} D_{\alpha,\beta}(\nabla_{\#}\partial_{\phi_{j,\alpha}})(\nabla_{\#}\partial_{\phi_{j,\beta}})\Bigg) \tag{71}$$

The linear functions evolve according to:

$$e^{L_0 t}\phi_{j,\alpha} = \sum_{j'=1}^{N}\sum_{\alpha'=1}^{n}(e^{tB})_{j\alpha,j'\alpha'}\phi_{j',\alpha'} \tag{72}$$

where $B = -\nabla_{\#}\otimes \text{ diag}(c_1, ..., c_n) - \nabla_{\#}\nabla_{\#}^T D$ with the reminder that $RAR^{-1} = \text{diag}(c_1, .., c_n)$.
Next we consider $\mathcal{N}_{j,\alpha} \neq 0$. This will modify the invariant measure in a sporadic

way that is difficult to study in general. Hence we choose to study the case of $\mathcal{N}_{j,\alpha}$ where ρ_G is left invariant under the deterministic flow generated by the evolution equation $\frac{d}{dt}\phi = -\nabla_{\#}\mathcal{N}$, that is, under the generator:

$$L_1 = -\sum_{j=1}^{N}\sum_{\alpha=1}^{n}\nabla_{\#}\mathcal{N}_{j,\alpha}\partial_{\phi_{j,\alpha}} \tag{73}$$

and so the invariance of ρ_G under L_1 is the same as the condition:

$$\sum_{j=1}^{N}\sum_{\alpha=1}^{n}\phi_{j,\alpha}\nabla_{\#}\mathcal{N}_{j,\alpha} \tag{74}$$

Now that we have identified the generator and invariant measure, we can analyse the stationary $\phi_{j,\alpha}(t)$ process governed by (67). Denote averages with respect to ρ_G by $\langle\cdot\rangle_{eq}$. Then for $t \geq 0$, the stationary covariance is:

$$S^{\#\phi}_{\alpha,\beta}(j,t) = \langle\phi_{j,\alpha}(t)\phi_{0,\beta}(0)\rangle = \langle\phi_{0,\beta}e^{Lt}\phi_{j,\alpha}\rangle_{eq} \tag{75}$$

Where $L = L_0 + L_1$ is the generator associated with (67). We will suppress the superscript $\#\phi$ on the correlator for easier reading because that is the only correlator we will refer to in this section. By construction

$$S_{\alpha,\beta}(j,0) = \delta_{\alpha,\beta}\delta_{j,0} \tag{76}$$

The time derivative is then

$$\frac{d}{dt}S_{\alpha,\beta}(j,t) = \langle\phi_{0,\beta}(e^{Lt}L_0\phi_{j,\alpha})\rangle_{eq} + \langle\phi_{0,\beta}(e^{Lt}L_1\phi_{j,\alpha})\rangle_{eq} \tag{77}$$

Plugging

$$e^{Lt} = e^{L_0t} + \int_0^t e^{L_0(t-s)}L_1e^{Ls}ds \tag{78}$$

into (77), the term with e^{L_0t} vanishes since it's cubic in the time zero fields $(\phi_j(0))$ and so the average $\langle\cdot\rangle_{eq}$ vanishes, Hence the time evolution becomes:

$$\frac{d}{dt}S_{\alpha,\beta}(j,t) = \sum_{j\in\mathbb{Z}}\sum_{\alpha'=1}^{n}\left(B_{\alpha j,\alpha' j'}S_{\alpha'\beta}(j',t) + \int_0^t ds\langle\phi_{0,\beta}e^{L_0(t-s)}L_1)e^{Ls}L_1\phi_{j,\alpha})\rangle_{eq}\right) \tag{79}$$

The adjoint of $e^{L_0(t-s)}$ is obtained from (72) and the adjoint of L_1 is obtained from

$$\langle\phi_{j,\alpha}L_1F(\phi)\rangle_{eq} = -\langle(L_1\phi_{j,\alpha})F(\phi)\rangle_{eq} \tag{80}$$

We also have that

$$L_1\phi_{j,\alpha} = -\nabla_{\#}\mathcal{N}_{j,\alpha} \tag{81}$$

Inserting $(72, 80-81)$ into (79), we obtain the identity:

$$\frac{d}{dt}S_{\alpha,\beta}(j,t) = \sum_{j\in\mathbb{Z}}\sum_{\alpha'=1}^{n}\Bigg(B_{\alpha j,\alpha' j'}S_{\alpha'\beta}(j',t) - \int_0^t ds(e^{B^T(t-s)})_{0\beta,j'\alpha'}\langle\nabla_{\#}\mathcal{N}_{j',\alpha'}(e^{Ls}\nabla_{\#}\mathcal{N}_{j,\alpha})\rangle_{eq}\Bigg) \tag{82}$$

We note that the average $\langle\nabla_{\#}\mathcal{N}_{j,\alpha}(s)\nabla_{\#}\mathcal{N}_{j',\alpha'}(0)\rangle$ in (82) is a 4-point correlation (that is, it is a functional average of a product of 4 field operators). Hence we can employ Gaussian factorization:

$$\langle\phi(s)\phi(s)\phi(0)\phi(0)\rangle \cong \langle\phi(s)\phi(s)\rangle\langle\phi(0)\phi(0)\rangle + 2\langle\phi(s)\phi(0)\rangle\langle\phi(s)\phi(0)\rangle \tag{83}$$

The first term on the right above vanishes once we plug in the difference operator $\nabla_{\#}$. The bare propagator $e^{B(t-s)}$ is replaced by the interacting propagator $S(t-s)$, combined with taking the continuum limit of $S(j,t)$ into $S(x,t)$, $x\in\mathbb{R}$ we obtain the mode-coupling equation:

$$\frac{d}{dt}S_{\alpha,\beta}(j,t) = \sum_{\alpha'=1}^{n}(-c_\alpha\delta_{\alpha\alpha'}\partial_x + D_{\alpha\alpha'}\partial_x^2)S_{\alpha'\beta}(x,t) + \int_0^t ds\int_{\mathbb{R}} dy\partial_y^2 M_{\alpha\alpha'}(y,s)S_{\alpha',\beta}(x-y,t-s) \tag{84}$$

with memory kernel:

$$M_{\alpha\alpha'}(x,t) = 2\sum_{\beta',\beta'',\gamma',\gamma''=1}^{n} G^{\alpha}_{\beta'\gamma'}G^{\alpha'}_{\beta''\gamma''}S_{\beta',\beta''}(x,t)S_{\gamma\gamma''}(x,t) \tag{85}$$

Going back to the BS model again and considering the diagonalization procedure (52) done in section 3 with:

$$S(x,t) \simeq \begin{pmatrix} f_1(x,t) & 0 \\ 0 & f_2(x,t)\end{pmatrix} \tag{86}$$

if $\beta'\neq\beta''$ then $S_{\beta',\beta''}\simeq 0$. Similarly, if $\gamma'\neq\gamma''$ then $S_{\gamma',\gamma''}\simeq 0$. Finally, since the modes are going in opposite directions, $f_1(x,t)f_2(x,t)\simeq 0$ for large t. This amounts to $S_{\gamma,\gamma}(x,t)S_{\beta,\beta}(x,t)\simeq 0$ for large t. Hence, when the appropriate diagonalization procedure is carried out, the memory kernel simplifies to

$$M_{\alpha\alpha'}(x,t) = \begin{cases} 2\sum_{\gamma=1}^{n}(G^{\alpha}_{\gamma\gamma})^2 S_{\gamma,\gamma}(x,t)^2 & \text{if } \alpha=\alpha' \\ 0 & \text{if } \alpha\neq\alpha'\end{cases} \tag{87}$$

4.1 Heat Mode Scaling for the Levy Case

In this section, we give an example of how (84) can be used to study the mode coupling behaviour of the two component stochastic Burgers equation. We use the example of the case that corresponds to Table 3 row 1 since it is a relatively easy example due to the symmetry involved. The calculations for other cases can be found in ([1], [2], [3]). The equation is of the form

$$\partial_t u_\sigma + \partial_x(\sigma c u_\sigma + \lambda(u_{-\sigma})^2 - D\partial_x\partial_\sigma + \sqrt{2D}\xi_\sigma = 0, \quad \sigma = \pm 1 \tag{88}$$

With the simplification that the strength of the non-linearity λ is the same for both modes. Here the index of the modes is ± 1 instead of $1, 2$ like in previous sections, and the frame of reference is such that the velocity of the modes are opposite. Using the mode coupling equations $(84-87)$, we obtain

$$\partial_t f_\sigma(x,t) = (-\sigma c\partial_x + D\partial_x^2) f_\sigma(x,t) + 2\lambda^2 \int_0^t \int_{\mathbb{R}} f_\sigma(x-y, t-s)\partial_y^2 (f_{-\sigma}(y,s)^2) dyds \tag{89}$$

with initial condition $f_\sigma(x, 0) = \sigma(x)$ and the normalization

$$\int_{\mathbb{R}} f_\sigma(x,t) = 1 \tag{90}$$

is preserved. By the symmetry of (89), we have

$$f_\sigma(x,t) = f_{-\sigma}(-x,t) \tag{91}$$

The goal is to find a self similar solution of (89). It will be shown that the space-time scaling is $x/t^{1/\gamma}$ where γ is the golden mean:

$$\gamma = \frac{1+\sqrt{5}}{2} \simeq 1.618 \tag{92}$$

The analysis is easier in Fourier space. We use the convention

$$\hat{g}(k) = \int_{\mathbb{R}} g(x) e^{-2i\pi kx} dx \tag{93}$$

Taking the Fourier transform of (89) yields

$$\begin{aligned}\partial_t \hat{f}_\sigma(k,t) = &- (2i\pi\sigma ck + (2\pi k)^2 D)\hat{f}_\sigma(k,t) \\ &- 2(2\pi k)^2\lambda^2 \int_0^t \hat{f}_\sigma(k, t-s)\big(\int_{\mathbb{R}} \hat{f}_{-\sigma}(k-q, s)\hat{f}_{-\sigma}(q,s)dq\big)ds\end{aligned} \tag{94}$$

We assume that relative to σct, f_σ is a self-similar solution. That is:

$$f(x,t) = t^{-a}F(t^{-a}(x \mp ct)) \tag{95}$$

Then in Fourier space, the scaling becomes:

$$\hat{f}(k,t) = \exp(\mp 2i\pi kct)\hat{F}(kt^a) \tag{96}$$

The following scaling ansatz is made:

$$\hat{f}_1(k,t) = \exp(-2i\pi kct)h(k^\gamma t), \quad \hat{f}_{-1}(k,t) = \exp(2i\pi kct)h(kt^\beta) \tag{97}$$

which is expected to be valid asymptotically (this statement is made precise in (104)). In (94), we consider g as the input and h as the output. This amounts to considering the forcing exerted by f_{-1} on f_1. Since f_σ is real valued, $h(-w) = \overline{h(w)}$ and $g(-w) = \overline{h(w)}$, so it suffices to only consider $k > 0$. Inputting (97) into (94), for f_1, we obtain:

$$\begin{aligned} k^\gamma h'(k^\gamma t) =& -(2\pi k)^2 D h(k^\gamma t) \\ & - 2(2\pi k)^2 \lambda^2 \int_0^t h(k^\gamma(t-s)) \int_{\mathbb{R}} g((k-q)s^\beta) g(qs^\beta) e^{4i\pi cks} dq ds \end{aligned} \tag{98}$$

Letting $w = k^\gamma t$, $u = qs^\beta$ (98) becomes

$$\begin{aligned} h'(w) =& -4\pi^2 D k^{2-\gamma} h(w) \\ & - 8\pi^2 \lambda^2 k^{2-\gamma} \int_0^{k^{-\gamma} w} s^{-\beta} h(w - k^\gamma s) e^{4i\pi cks} \int_{\mathbb{R}} g(ks^\beta - u) g(u) du ds \end{aligned} \tag{99}$$

Rescaling the time integration variable as $s = k^{-a}\theta$ yields

$$\begin{aligned} h'(w) =& -4\pi^2 D k^{2-\gamma} h(w) \\ & - 8\pi^2 \lambda^2 k^{2-\gamma+a(\beta-1)} \int_0^{k^{a-\gamma} w} \theta^{-\beta} h(w - k^{\gamma-a}\theta) e^{4i\pi ck^{1-a}\theta} \int_{\mathbb{R}} g(k^{1-a\beta}\theta^\beta) g(u) du d\theta \end{aligned} \tag{100}$$

As $k \to 0$, $a = 1$ is the only choice for a leading to a non trivial integral over θ. If $a < 1$, the exponential factor converges to 1 and so the integrand is proportional to $\theta^{-\beta}$ which is not integrable over $\mathbb{R}_+$. If $a > 1$, the integral converges to 0 since the exponential factor oscillates wildly. Setting

$$\gamma = 1 + \beta, \quad 0 < \beta < 1 \tag{101}$$

and $a = 1$, we obtain:

$$\begin{aligned} h'(w) =& -4\pi^2 D k^{2-\gamma} h(w) \\ & - 8\pi^2 \lambda^2 \int_0^{k^{1-\gamma} w} \theta^{-\beta} h(w - k^\beta \theta) e^{4i\pi c\theta} \int_{\mathbb{R}} g(k^{1-\beta}\theta^\beta) g(u) du d\theta \end{aligned} \tag{102}$$

in the limit $k \to 0$:

$$h'(w) = -h(w)(4\pi\lambda)^2 \left(\int_0^\infty |g(u)|^2 du \right) \left(\int_0^\infty e^{4i\pi c\theta} \theta^{-\beta} d\theta \right) \tag{103}$$

Once the values of the integrals on the right hand side are known, the above determines h. We can now state precisely the limiting procedure:

$$\lim_{k\to 0} e^{2i\pi ck^{1-\gamma}w}\hat{f}_1(k,k^{-\gamma}w) = h(w), \tag{104}$$

where h is a solution of (103). The time integral in (103) is computed in analytically in [4]:

$$\int_0^\infty e^{4i\pi c\theta}\theta^{-\beta}d\theta = (4\pi c)^{-1+\beta}\int_0^\infty e^{is}s^{-\beta}ds = a\Big(1+\frac{i}{\tan(\pi\beta/2)}\Big) \tag{105}$$

where

$$a = (4\pi c)^{-1+\beta}\frac{\pi}{2\Gamma(\beta)\cos(\pi\beta/2)} \tag{106}$$

If we repeat the above derivation but consider h as the input and g as the output, by symmetry, we obtain:

$$h(k^\gamma t) = \overline{g((k^{1/\beta}t)^\beta)} \tag{107}$$

which forces $h(w) = \overline{g(w^\beta)}$ and

$$\gamma = 1/\beta \tag{108}$$

Now (101) and (108) imply that γ is the golden mean (92). The normalization (90) implies $h(0) = 1$. Using $\tan(\pi\beta/2) = -1/\tan(\pi\gamma/2)$, we obtain:

$$h(w) = \exp(-(r\pi\lambda)^2 a(1-i\tan(\pi\gamma/2))Aw) \tag{109}$$

where

$$A = \int_0^\infty |g(u)|^2du = \int_0^\infty |h(w^\gamma)|^2dw \tag{110}$$

but since we know h from (109), we can insert it into A above to get:

$$A = (a(r\pi\lambda)^2)^{-1/\gamma^2}\tilde{A}^{1/\gamma}, \quad \tilde{A} = \int_0^\infty e^{-w^\gamma}dw = \frac{2^{-1/\gamma}}{\gamma}\Gamma(1/\gamma) \tag{111}$$

So finally, we obtain the solution from (97):

$$\hat{f}_\sigma(k,t) = \exp(-2i\pi\sigma kct - C|2\pi k|^\gamma(1-i\sigma\,\mathrm{sgn}(k)\tan(\pi\gamma.2))t) \tag{112}$$

with

$$C = \frac{1}{2}\lambda^{2/\gamma}\Big(\frac{1}{\gamma\sin(\pi\gamma/2)}\Big)^{1/\gamma}c^{1-2/\gamma} \tag{113}$$

Now (112) is the Fourier transform of an α-stable law with $\alpha = \gamma$ and symmetry parameter σ. The properties of this law are given in the next section.

4.2 The Levy Distribution

The levy distribution is defined through it's Fourier transform as:

$$f_{\mathrm{Levy},\alpha,b} = \frac{1}{2\pi}\int_{\mathbb{R}} \varphi_{\alpha,b}(k)e^{ikx}dk, \ \ \varphi_{\alpha,b}(k) = \exp\big(-|k|^{\alpha}[1 - ib\tan(\pi\alpha/2)\mathrm{sgn}(k)]\big) \tag{114}$$

Where the two parameters are $0 < \alpha < 2$ and $|b| \leq 1$. α controls the steepness and b controls the asymmetry. For the case above, we have maximal asymmetry $b = \pm 1$, and $\alpha = \gamma$, we have that the decay is like $\exp(-c_0 x^{\alpha/(1-\alpha)})$ where c_0 is a known constant. More details about this and other relevant distributions are found in [4].

5 Numerical Analysis

To asses the validity of the mode scaling $(64 - 65)$, the dynamics of the BS (13) model is numerically simulated including the random nearest neighbour exchanges. The numerical simulation is done for two sample potentials: the first being the $FPU - \alpha$ potential

$$V(\eta) = \frac{1}{2}\eta^2 + \frac{a}{3}\eta^3 + \frac{1}{4}\eta^4 \tag{115}$$

with $a = 2$ and the Kac-Van-Moerbeke (KvM) potential

$$V(\eta) = \frac{e^{-\kappa\eta} + \kappa\eta - 1}{\kappa^2} \tag{116}$$

with $\kappa = 1$. In order to ensure the convergence of the normalization constant (18) in the canonical measures, $\tau > -1/\kappa$ is necessary.

The initial conditions are sampled according to the canonical measure (41). The initial values $(\eta_{i,0})_{i=0,\ldots,N-1}$ can be sampled independently according to (41) since the measure is of product form.

The dynamics of (13) are integrated using an algorithm available in section 6.3.1 of [3] adapted to the periodic conditions. The algorithm integrates the even and odd sites η_i separately according to the deterministic part of the dynamics using time step $\Delta t > 0$. As for the random part of the dynamics, each pair in $\{(\eta_0, \eta_1), ..., (\eta_{N-1}, \eta_0)\}$ is assigned an independent exponential clock (sampled with mean $1/\gamma$ which is decreased by Δt at each time step. When a clock becomes negative, the corresponding neighbouring displacements are exchanged and a new clock is sampled.

Since the goal is to verify the structure of the correlator, we must compute it empirically. K samples of initial conditions are produced with initial conditions

$\eta^k_{i,0}$. Then the empirical volume and energy at each site i can be computed as follows:

$$\overline{h}_{i,n} = \frac{1}{K}\sum_{k=1}^{K}\eta^k_{i,n}, \quad \overline{e}_{i,n} = \frac{1}{K}\sum_{k=1}^{K}V(\eta^k_{i,n}) \tag{117}$$

Hence the empirical correlation matrix can be computed by the following:

$$[C_{N,K}] = \frac{1}{KN}\sum_{k=1}^{K}\sum_{i=1}^{N-1}u^k_{\alpha,i+j,n}u^k_{\alpha',j,0} \tag{118}$$

where

$$u_{1,i,m} = \eta^k_{i,m} - \overline{h}_{i,m}, \quad u_{2,i,m} = V(\eta^k_{i,m}) - \overline{e}_{i,m} \tag{119}$$

With values of $K = 10^5$, and lengths N between 2000 and 8000, and timestep $\Delta t = 0.005$, it was verified that

$$C^{\#}_{N,K}(i,n) = RC_{N,K}(i,n)R^t \simeq \begin{pmatrix} f_1^{num}(i,n) & 0 \\ 0 & f_2^{num}(i,n)\end{pmatrix} \tag{120}$$

The last order of business is to compare f_α^{num} with the ansatz f_α in $(64-65)$. This is done by minimizing the the L^1 distance between the functions by optimizing the scaling parameters. Specifically, the following is numerically minimized:

$$\inf_{\substack{x_n\in\mathbb{R}\\ \Lambda_n>0}}\left\{\sum_{i=0}^{N-1}|f_\alpha^{num}(i,n) - (\Lambda_n)^{-1}f_\alpha^{mc}((\Lambda_n)^{-1}(i-x_n))|\right\} \tag{121}$$

where f_α^{mc} is the predicted theoretical scaling function, that is KPZ for $\alpha = 1$ and maximally asymmetric $\frac{5}{3}-$Levy for $\alpha = 2$. To increase the rate of convergence and stability of the optimization, prior knowledge is used to write:

$$x_n = c_{\text{theor}}n\Delta t + \tilde{x}_n, \quad \Lambda_n = \tilde{\Lambda}_n(n\Delta t)^{\delta_{\text{theor}}} \tag{122}$$

Where max speed c_{theor} corresponds to the eigenvalue of A for the mode in question. That is $c_{\text{theor}} = 2(\partial_v - \tau\partial_e)\tau$ for the sound mode and $c_{\text{theor}} = 0$ for the heat mode. δ_{theor} is the predicted scaling exponent, that is $\delta_{\text{theor}} = 2/3$ for the sound mode and $\delta_{\text{theor}} = 5/3$ for the heat mode. The optimization above is now done over $\tilde{x}_n$ and $\tilde{\Lambda}_n$. These values could be drifting in time when the expected scaling (122) is not exact, which is inevitable due to discrete time step. Hence in the numerical simulation, it could be that the modes are not travelling with exact speeds of c_{theor}. Therefore $\tilde{x}_n$ and $\tilde{\Lambda}_n$ are fit using

$$\tilde{x}_n = c_{\text{crt}}n\Delta t + x_0, \quad \tilde{\Lambda}_n = \tilde{\Lambda}_0(n\Delta t)^{\delta_{\text{crt}}} \tag{123}$$

Where the numerical velocity observed is $c_{\text{num}} = c_{\text{theor}} + c_{\text{crt}}$ and the scaling exponent observed is $\delta_{\text{num}} = \delta_{\text{theor}} + \delta_{\text{crt}}$. The fits on $\tilde{x}_n$ and $\tilde{\Lambda}_n$ above are obtained by least square minimization on $\tilde{x}_n$ and $\log \tilde{\Lambda}_n$ respectively. In all cases, x_0 is found to be very small and is set to 0. Finally the scaling factor is obtained by:

$$\lambda_{\text{num}} = \tilde{\Lambda}_0^{1/\delta_{\text{num}}} \tag{124}$$

We can also have a notion of an instantaneous estimate of a scaling factor by

$$\lambda_n = \left(\tilde{\Lambda}_n (n\Delta t)^{-\delta_{\text{crt}}}\right)^{1/\delta_{\text{num}}} \tag{125}$$

In the following figures, a rescaled peak plot is a plot for which the renormalized numerical correlation functions $(\lambda_{\text{num}} n\Delta t)^{\delta_{\text{num}}} f_\alpha^{num}(i,n)$ as a function of the renormalized spatial variable $(i - c_{\text{num}} n\Delta t)/(\lambda_{\text{num}} n\Delta t)^{\delta_{\text{num}}}$. The results displayed in this section were obtained with the following parameters: a temperature $\beta^{-1} = \frac{1}{2}$, tension $\tau = 1$, and noise intensity $\gamma = 1$.

5.1 Numerical Results for FPU Potential

The numerical parameters obtained by the minimization procedure are as follows:

Sound Peak: δ_{num} turns out to be extremely close to 2/3 as predicted. The velocity obtained is $c_{\text{num}} = -5.24$ as compared to the predicted value $c_{\text{theor}} = -5.28$. The scaling value obtained is $\lambda_1 \simeq 6.36$ which is close to the predicted value $\lambda_1 = 2\sqrt{2}|G_{11}^1| = 6.32$ as in (64).

Heat Peak: The reference distribution is a maximally asymmetric Levy distibution with $\alpha = 5/3$. The velocity being c_{num} is very close to 0 as expected. The exponent $\delta_{\text{num}} = 0.605$ is close to the predicted value of 3/5. The numerical scaling factor obtained was $\lambda_2 \simeq 3.70$ compared to the predicted value $\lambda_2 = a_h c^{-1/3} (G_{11}^2)^2 \lambda_1^{-2/3} = 3.46$ as in (65).

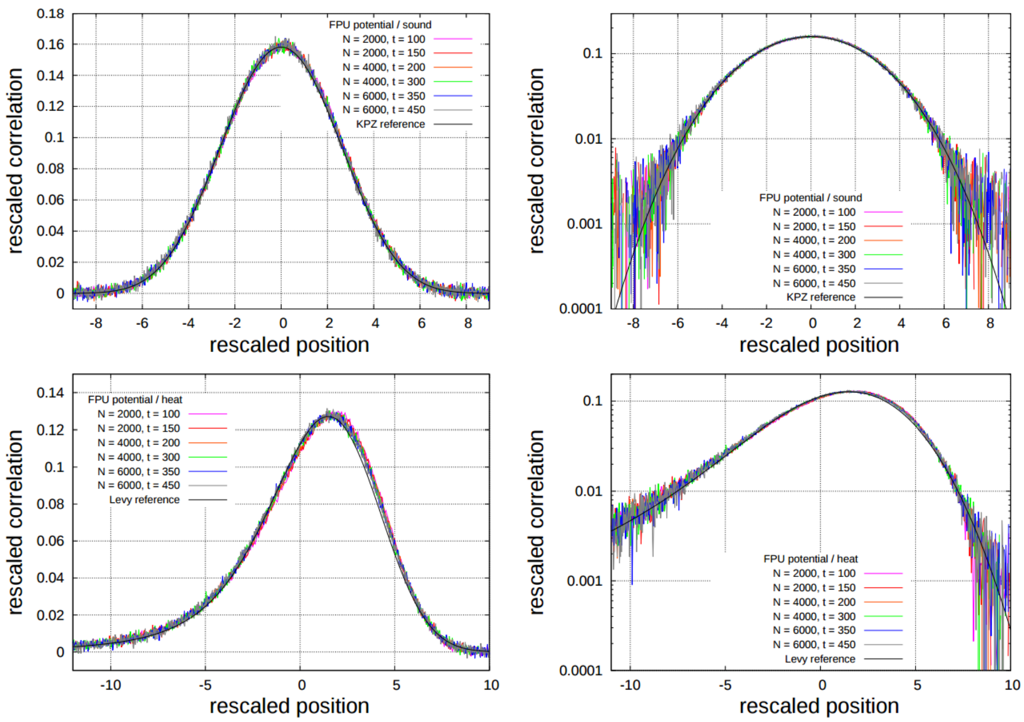

Figure 1: This image shows a comparison of the rescaled sound and heat peaks for the FPU potential. The first row corresponds to the sound peak, and the second row corresponds to the heat peak. The second column plots the peaks in the first column in a logarithmic scale.

Also related to this section are figures showing the evolution of the non-universal scaling factors as a function of the time index. The L^1 error decreases quickly in the beggining, but after reaching a minimum, slowly increases due to the increase in the statiscal noise. The initial decrease is faster for the sound peak because it attains its asymptotic shape quicker.

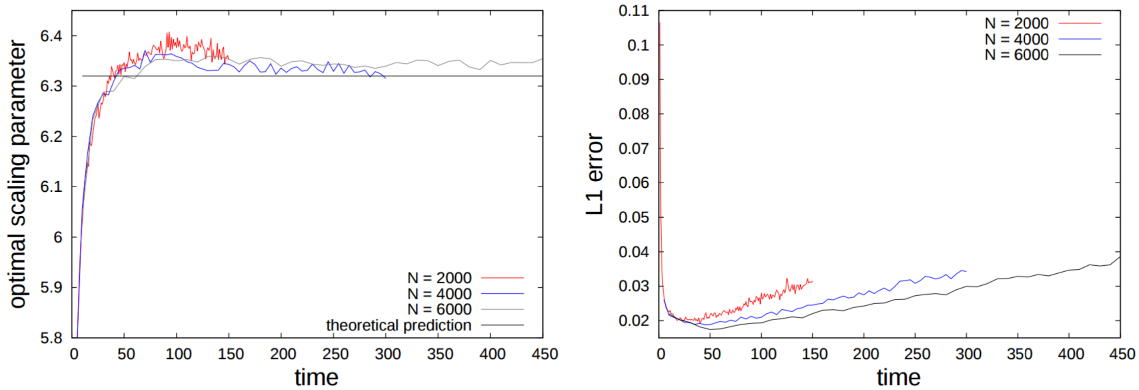

Figure 2: FPU potential sound peak. The left plot shows the evolution of the optimal value of the scaling parameter as given by (125). On the right is the L^1 error for the optimal value of the parameters given by (121).

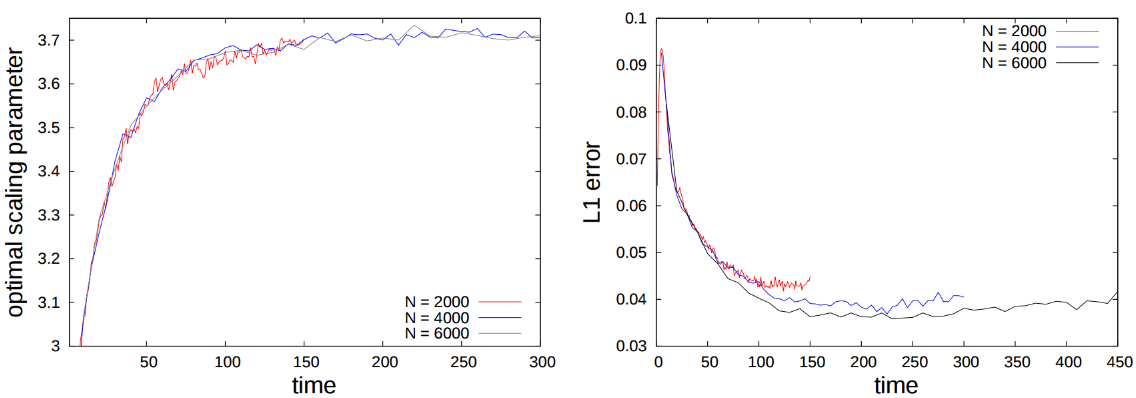

Figure 3: FPU potential heat peak. The left plot shows the evolution of the optimal value of the scaling parameter as given by (125). On the right is the L^1 error for the optimal value of the parameters given by (121).

5.2 Numerical Results for KvM Potential

The numerical parameters obtained by the minimization procedure are as follows:
Sound Peak: δ_{num} turns out to be extremely close to 2/3 as predicted. The velocity obtained is $c_{\text{num}} = -3.996$ as compared to the predicted value $c_{\text{theor}} = -4$. The scaling value obtained is $\lambda_1 \simeq 2.81$ which is close to the predicted value $\lambda_1 = 2\sqrt{2}|G^1_{11}| = 2.83$ as in (64).

Heat Peak: The reference distribution is a maximally asymmetric Levy distibution with $\alpha = 1.57$ instead of $5/3$ since this value decreases the error (121). The velocity being c_{num} is very close to 0 as expected. The exponent $\delta_{\mathrm{num}} = 0.63$ which is somewhat near the predicted value of $3/5$. The numerical scaling factor obtained was $\lambda_2 \simeq 2.51$ which is far from the predicted value $\lambda_2 = a_h c^{-1/3} (G_{11}^2)^2 \lambda_1^{-2/3} = 4.21$ as predicted by (65).

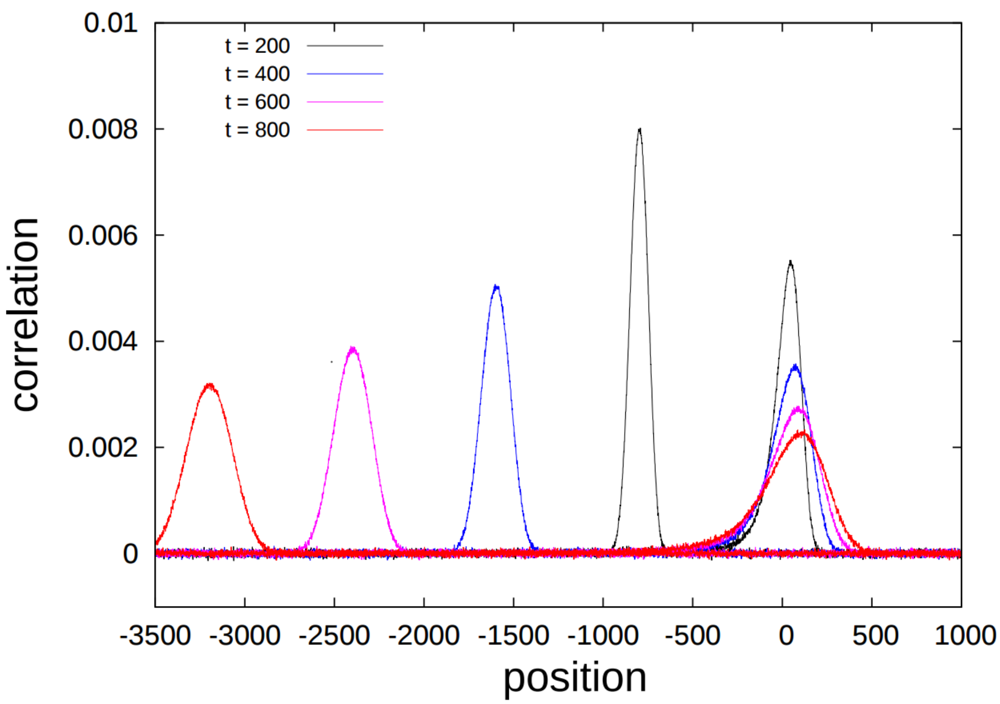

Figure 4: The above image shows the time evolution of the sound peak (f_1^{mc}) travelling to the left and the heat peak (f_2^{mc}) centered at $x = 0$ for the KvM potential. It is interesting to note that the rapid decay of the heat peak is in a direction away from the sound peak, so that its asymmetric.

Also related to this section are figures showing the evolution of the non-universal scaling factors as a function of the time index. We see similar results to the previous section. Again convergence for the sound peak is quicker.

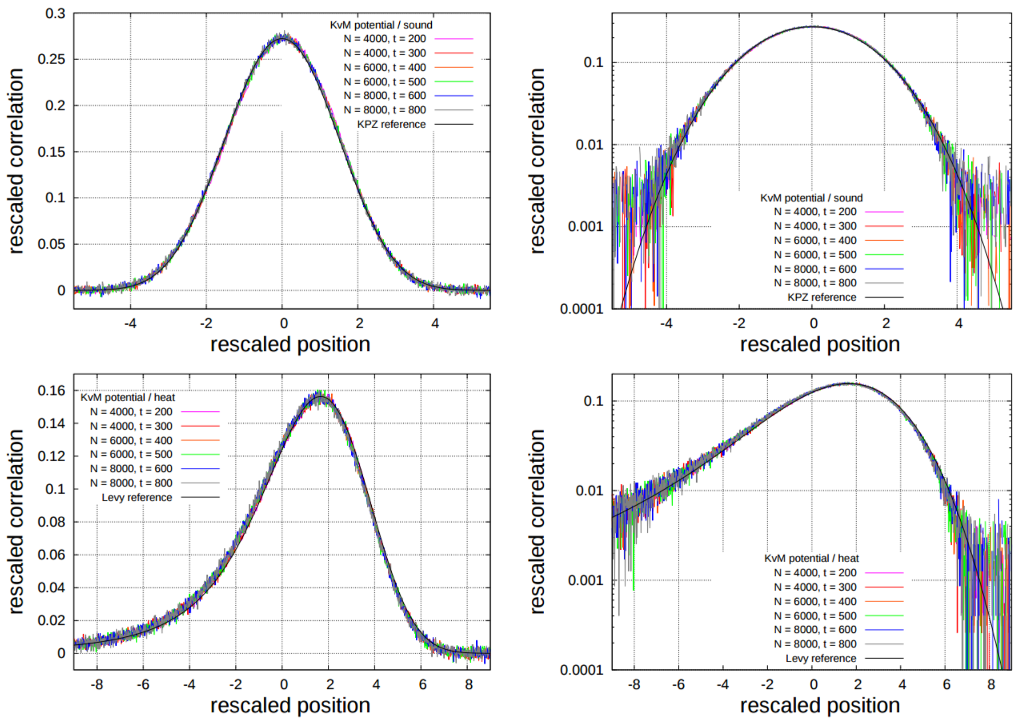

Figure 5: This image shows a comparison of the rescaled sound and heat peaks for the KvM potential. The first row corresponds to the sound peak, and the second row corresponds to the heat peak. The second column plots the peaks in the first column in a logarithmic scale.

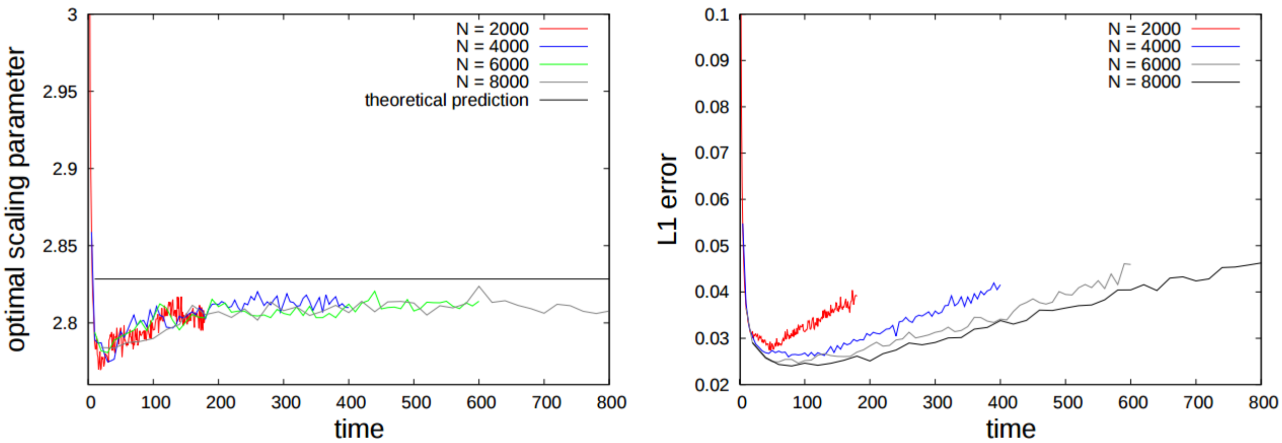

Figure 6: KvM potential sound peak. The left plot shows the evolution of the optimal value of the scaling parameter as given by (125). On the right is the L^1 error for the optimal value of the parameters given by (121).

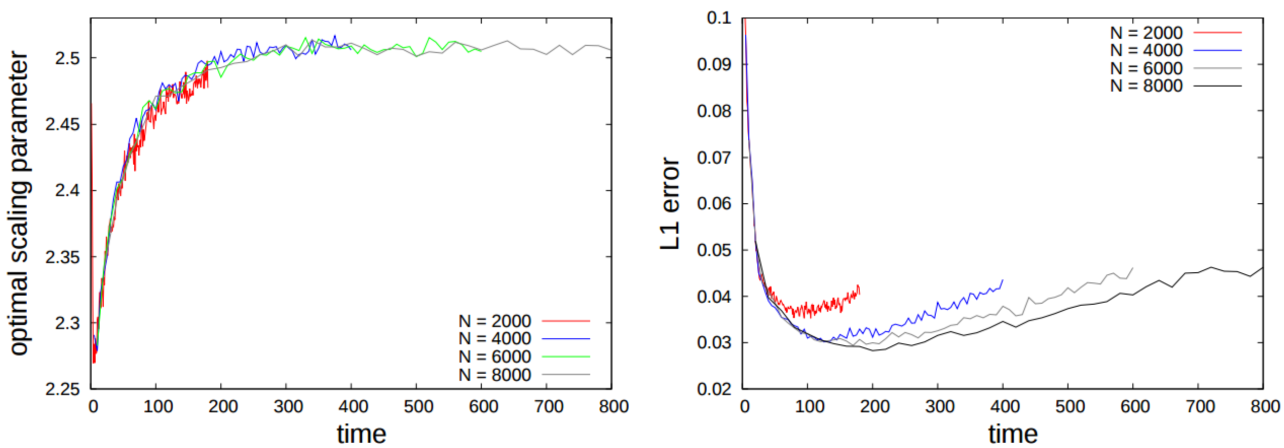

Figure 7: KvM potential heat peak. The left plot shows the evolution of the optimal value of the scaling parameter as given by (125). On the right is the L^1 error for the optimal value of the parameters given by (121).

6 Conclusion

We have walked through the process of understanding the behaviour of the equilibrium time correlations of the conserved fields using strategies of non-linear fluctuating hydrodynamics. Other models have been found which exhibit different universality classes, for instance in [10] both correlation functions are KPZ. In [11], both peaks are generally KPZ, but other universality classes can be realized. In [12], many more universality classes are realized including the *gold*-Levy class highlighted in section 4. As more models are being discovered for each universality class, non-linear fluctuating hydrodynamics proves itself to be an incredible tool for studying the behaviour of these anharmonic chain models.

References

[1] H. Spohn, Nonlinear fluctuating hydrodynamics for anharmonic chains. J. Stat. Phys. 154, 1191–1227 (2014).

[2] H. Spohn, Nonlinear fluctuating hydrodynamics for anharmonic chains. J. Stat. Phys. 154, 1191–1227 (2014).

[3] C. Bernardin and G. Stoltz, Anomalous diffusion for a class of systems with two conserved quantities. Nonlinearity 25, 1099–1133 (2012).

[4] D. Zwillinger, CRC Standard Mathematical Tables and Formulae (31st ed.) (CRC Press, 2003).

[5] T. Funaki and J. Quastel, KPZ equation, its renormalization and invariant measures. arXiv:1407.7310 (2014).

[6] A. Borodin, I. Corwin, P. Ferrari, and B. Veto, Height fluctuations for the stationary KPZ equation. arXiv:1407.6977 (2014).

[7] T. Imamura and T. Sasamoto, Stationary correlations for the 1D KPZ equation. J. Stat. Phys. 150, 908–939 (2013).

[8] M. Prahofer, Exact scaling functions for one-dimensional stationary KPZ growth. http://www-m5.ma.tum.de/KPZ

[9] Ch. B. Mendl and H. Spohn, Dynamic correlators of Fermi-Pasta-Ulam chains and nonlinear fluctuating hydrodynamics. Phys. Rev. Lett. 111, 230601 (2013).

[10] C. Bernardin, P. Gon¸calves, and M. Jara, 3/4-superdiffusion in a system of harmonic oscillators perturbed by a conservative noise. arXiv:1402.1562 (2014).

[11] V. Popkov, J. Schmidt, and G. M. Schutz, Superdiffusive modes in two-species driven diffusive systems. Phys. Rev. Lett. 112, 200602 (2014).

[12] V. Popkov, J. Schmidt, and G. M. Schutz, Universality classes in two-component driven diffusive systems. preprint (2014).